

PAWLEY, G. S. & WILLIS, B. T. M. (1970). *Acta Cryst.* **A26**, 260–262.  
 PRICE, P. F. & MASLEN, E. N. (1978). *Acta Cryst.* **A34**, 173–183.  
 STEWART, R. F. (1969). *J. Chem. Phys.* **51**, 4569–4577.

STEWART, R. F. (1970). *J. Chem. Phys.* **53**, 205–213.  
 STEWART, R. F. (1972). *Acta Cryst.* **A28**, S7.  
 STEWART, R. F. (1973a). Private communication.  
 STEWART, R. F. (1973b). *J. Chem. Phys.* **58**, 1668–1676.  
 STEWART, R. F. (1973c). *J. Chem. Phys.* **58**, 4430–4438.

*Acta Cryst.* (1978). **A34**, 203–216

## Electron-Density Studies.

### V. The Electron Density in Melamine (2,4,6-Triamino-*s*-triazine) with and without Exponent Refinement

BY P. F. PRICE, J. N. VARGHESE AND E. N. MASLEN

*Department of Physics, University of Western Australia, Nedlands, Western Australia*

(Received 13 December 1976; accepted 8 August 1977)

The electron density distribution in melamine has been studied with X-ray diffraction data and neutron structural parameters. The at-rest valence density is represented as a set of nuclear-centred multipole density functions with Slater-type radial functions. Two series of analyses were compared, the first with the radial exponents fixed at the standard molecular values and the second with these exponents as variable parameters. Exponent refinement allows a marked improvement in the fit of the model to the data. The population coefficients of the multipole terms are better defined when the exponents are optimized. On chemically similar atoms the populations of the monopole terms are inversely related to the exponents. The carbon atom parameters agree to high precision. Exponents for the ring and amine nitrogens differ and small differences within each set are related to the hydrogen-bond and packing environment. The exponents and electron density near the nucleus are relatively low for hydrogens involved in hydrogen bonding. The most significant deformation functions in the multipole expansion have a symmetry compatible with nearest-neighbour geometry. Differences between populations are related to distortions from the idealized geometry or to hydrogen-bonding interactions. The inclusion of a hydrogen dipole deformation term with a large exponent results in internally consistent populations which are correlated with N–H stretching amplitudes in the structure. This suggests that the convolution approximation is invalid at this level of structure refinement.

#### Introduction

The free molecule of 2-4-6-triamino-*s*-triazine (melamine) has  $6m2$  symmetry. Each of the carbon and nitrogens has  $mm2$  symmetry and the hydrogen atoms have symmetry  $m$ . In the crystal structure, which was first studied with X-ray data by Hughes (1941), there is one molecule in the asymmetric unit. The structure has since been more accurately determined with both X-ray and neutron data, by Varghese, O'Connell & Maslen (1977). A diagram of the structure is given in Fig. 1.

The unit cell is roughly equi-dimensional. The lack of a short cell dimension is a considerable advantage for charge-density analysis. In each principal direction there are points close to the origin of reciprocal space, where the contribution of the valence-electron density to the scattering is maximal. The parameters which determine the charge density can be determined to far higher accuracy than those for a smaller structure with data of comparable quality.

The symmetry of the free molecule is expected to persist approximately in the crystal. At this level of approximation the carbon and nitrogen atoms in the structure are equivalent in threes and the hydrogen atoms in sixes. This provides an internal check on the validity of the results.

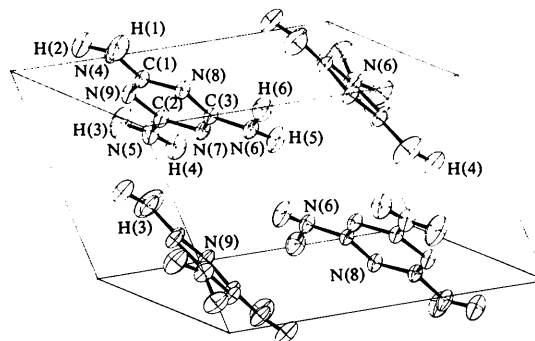


Fig. 1. Diagram of the melamine structure based on the neutron parameters of Varghese, O'Connell & Maslen (1977).

The atoms which are equivalent to first order are differentiated by hydrogen bonding and packing forces. The packing in the structure has been described by Varghese, O'Connell & Maslen (1977). Of the six hydrogens only H(1), H(2), H(4) and H(6) are involved in hydrogen bonding. H(6) is rather tightly packed in the structure with two close intermolecular contacts in addition to the hydrogen bond. The forces on H(6) have the effect of distorting the geometry around the amine nitrogen N(6). Whereas the amine groups at N(4) and N(5) are close to planar that at N(6) is semi-pyramidal, as is clearly shown in Fig. 1. N(4) is the donor nitrogen for two hydrogen bonds, whereas N(5) and N(6) are donors for one only. Of the ring nitrogens N(8) is the acceptor for two hydrogen bonds, whereas N(7) and N(9) are acceptors for one only.

Price, Maslen & Delaney (1978) have recently compared a number of charge-density models in a study of *s*-triazine. Models including 'two-centre' density functions, such as sets of orbital products constructed from *s* and *p* type functions, resulted in poorly defined parameters. The 'bond-directed scattering factor' model was not sufficiently flexible to describe the approximately trigonal charge distortion around the carbon and nitrogen atoms. The 'at rest valence density' (multipole density functions) model of Stewart (1972, 1973a) was found to be sufficiently flexible and yet had reasonably well defined parameters. It provided a good fit to the data if the radial exponents,  $\zeta_r$ , of the valence-density functions were optimized. This supported an earlier result by Stewart (1973b) in an analysis of the charge density in diamond. Preliminary calculations on melamine confirmed the generality of these observations, and only the results using one-centre multipole expansions are reported.

### Theoretical calculations

A semi-empirical INDO calculation was carried out, with the geometry determined by the neutron diffraction experiment (Varghese, O'Connell & Maslen, 1977). The resulting 'valence populations' (gross Mulliken atomic populations less two for C and N atoms) are shown in Table 1 together with those of two other semi-empirical (Santry, 1974) and one *ab initio* calculation (Chandler & Spackman, 1975). The other semi-empirical calculations were of CNDO/2 type, the first of the isolated molecule and the second including an allowance for crystalline field and intermolecular effects by a perturbation method (Bacon & Santry, 1971). The *ab initio* calculation was a STO-3G calculation with exponents fixed at the standard molecular values of Hehre, Stewart & Pople (1969). These calculations also used the above experimental geometry.

In the CNDO/2 (crystal field) calculations the populations of the hydrogen-bonded hydrogen atoms,

H(1), H(2), H(4) and H(6), are on average 0.023 e lower than those of H(3) and H(5), which are not involved in hydrogen bonds. Likewise the population of N(8) is 0.004 e larger than the mean of the N(7) and N(9) populations, and that of N(4) is 0.011 e greater than that of N(5). These changes correspond to involvement in two and one hydrogen bonds in each case. The population of N(6) is in turn 0.005 e lower than that of N(5) but each is involved in only one hydrogen bond.

### Experimental analyses

The experimental analyses were based on the 'at rest valence density' model. This makes use of the convolution approximation to write the thermally averaged molecular electron density as a sum of independently vibrating atom-like fragments, or 'pseudo-atoms'. The pseudo-atom is described as the sum of core and valence terms. The core density for a first row atom was calculated from the 1s wavefunction of the atom in the ground state, as tabulated by Clementi (1965). The valence density is written as a sum of nuclear-centred density functions with the angular form of the surface harmonics (multipoles) and of exponential radial form. In principle, a population parameter and

Table 1. Mulliken gross valence populations

The 'charge density' results from four recent semi-empirical and small basis set *ab initio* theoretical calculations. Geometries were from the neutron diffraction study of Varghese, O'Connell & Maslen (1977). CNDO – a CNDO/2 calculation by Santry (1974). Cryst. – a CNDO/2 calculation including intermolecular effects by a perturbation method (Santry, 1974). INDO – an INDO calculation by Varghese (1974). STO-3G (SM) – an STO-3G calculation with standard molecular exponents by Chandler & Spackman (1975)

Atom	CNDO	Cryst.	INDO	STO-3G (SM)
H(1)	0.880	0.859	0.88	0.78
H(2)	0.882	0.864	0.88	0.78
H(3)	0.882	0.880	0.88	0.78
H(4)	0.881	0.853	0.88	0.78
H(5)	0.896	0.891	0.90	0.79
H(6)	0.896	0.874	0.90	0.80
Mean	0.89	0.87	0.89	0.78
C(1)	3.622	3.616	3.54	3.66
C(2)	3.619	3.613	3.54	3.65
C(3)	3.625	3.619	3.54	3.67
Mean	3.62	3.62	3.54	3.66
N(4)	5.243	5.271	5.25	5.41
N(5)	5.240	5.260	5.24	5.41
N(6)	5.232	5.255	5.25	5.41
Mean	5.24	5.26	5.25	5.41
N(7)	5.366	5.379	5.44	5.36
N(8)	5.367	5.384	5.44	5.36
N(9)	5.368	5.381	5.44	5.36
Mean	5.37	5.38	5.44	5.36

radial exponent term can be determined for each multipole. The normalization of the density functions is such that the population of the monopole term equals the number of electrons it contains while those of the other multipoles equal the number of electrons transferred from the negative regions to the positive regions of the functions.

Because of the limitations of the model, the sum of the monopole populations will not necessarily equal the number of electrons in the molecule. A projection parameter,  $P$ , can be defined as the ratio of the experimental to the true number of electrons in the molecule, and should be an indicator of the sampling completeness of the density-function basis.

The details of this model and of the definition of the projection parameter were given by Price, Maslen & Delaney (1978).

In the following analyses the atomic positions and thermal parameters were held fixed at the values determined from the neutron diffraction experiment of Varghese, O'Connell & Maslen (1977). The refinement was based on the X-ray data of the same authors. This is an extensive set of 3315 accurate reflections collected on a Picker FACS1 automatic diffractometer at the University of Goteborg in Sweden. Data was collected to an angle of  $2\theta = 68^\circ$  with Mo  $K\alpha$  radiation, with the maximum value of  $\sin \theta/\lambda = 0.90 \text{ \AA}^{-1}$ . The least-squares weights were derived from counting statistics alone. The refinement was on the structure factors,  $F(\mathbf{S})$ .

The final refinement statistics were  $R_w = 0.048$ ,  $R = 0.056$  and  $\text{GoF} = 4.90$  (7).\* The GoF as a function of angle varied between 25.1 for  $|\mathbf{S}|$  in the range 0.0 to 0.1, and 2.5 for the high-angle data.

The internal agreement factor  $R_w(I) = \sum w_i |\Delta I| / \sum w_i I_{\text{av}}$ , where  $w_i$  is the reciprocal of the variance for the intensity,  $\Delta I$  is the difference in intensity for two equivalents and  $I_{\text{av}}$  the average value, was 0.039 for the equivalents which were measured. Standard deviations in the intensities estimated from the agreement between equivalents were in the range 1.0 to 1.2 times the counting-statistics values for the moderate to weak reflections which constitute the bulk of the data. For the few strong reflections the ratio of these e.s.d.'s was 6.0.

For a set of X-ray structure factors based on neutron structural parameters with atomic X-ray scattering factors the agreement statistics were  $R_w = 0.077$ ,  $R = 0.113$  and  $\text{GoF} = 7.42$  (10).

\* The refinement indices  $\text{GoF}$ ,  $R_w$  and  $R$  are defined as:

$$\begin{aligned} \text{GoF} &= [\sum_i w_i (\Delta F_i)^2 / (n - m)]^{1/2} \\ R_w(F) &= [\sum_i w_i (\Delta F_i)^2 / \sum_i w_i F_{i,\text{obs}}^2]^{1/2} \\ R(F) &= \sum_i |\Delta F_i| / \sum_i F_{i,\text{obs}} \end{aligned}$$

where  $w_i = \sigma_i^{-2}$  is the weight of the  $i$ th observed structure factor,  $F_{i,\text{obs}}$ ;  $F_{i,\text{calc}}$  is the calculated value of the  $i$ th structure factor;  $\Delta F_i = F_{i,\text{obs}} - F_{i,\text{calc}}$ ;  $n$  is the number of structure factors (3315), and  $m$  is the number of parameters in the model.

An isotropic extinction correction given by the formula of Zachariasen (1967) was applied in each analysis.

### Coordinate system

Since true site symmetry of the atoms in the melamine structure is 1, the symmetry does not forbid any of the surface harmonics in an atom-centred expansion of the density. However, classical bonding concepts and the evidence of  $X - N$  difference density maps suggest that those distortion terms describing the approximate symmetry of the bonds will be dominant. Hence, it is desirable to choose coordinate systems for the atoms such that the positive lobes of certain multipoles lie as closely as possible to the bonding directions.

If the nitrogen lone-pair directions are treated as equivalent to the bonding directions, if all bonds on one atom are treated as equivalent, and if the differences between bond angles are neglected, then the carbon and nitrogen atoms are in a trigonal bonding environment and the approximate site symmetry is  $\bar{6}m2$ . Neglecting second-nearest-neighbour interactions, the charge distortion on the hydrogen atoms is expected to be cylindrically symmetrical along the N-H bonds.

The following atomic-coordinate scheme was thus chosen: for each carbon and nitrogen atom, the  $\mathbf{z}$  direction is orthogonal to the least-squares plane through the atom itself and the neighbours to which it is bonded. For the carbon atoms the  $\mathbf{x}$  direction lies as near as possible to the bond direction between the carbon and the amine nitrogen, *i.e.* orthogonal to  $\mathbf{z}$  but in the plane of  $\mathbf{z}$  and the C-N(amine) vector. Similarly, for the amine nitrogens, the  $\mathbf{x}$  direction is as near as possible to the direction of the N-C bond. For the ring nitrogens the  $\mathbf{x}$  direction is in the opposite direction to the bisector of the C-N-C bond angle, which is hopefully the lone-pair direction. For the hydrogen atoms, the  $\mathbf{z}$  direction is along the H-N bond, and the  $\mathbf{x}$  direction is orthogonal to  $\mathbf{z}$  and as nearly orthogonal to the least-squares plane through the amine group and the associated carbon atom as possible (*i.e.* the  $zx$  plane contains the perpendicular to this plane). Fig. 2 depicts this coordinate system in an idealized manner.

With this coordinate system the distortion terms expected to be dominant are, for the heavy atoms, the trigonal octupole  $O_1$ , with its three positive lobes pointing approximately along the bonding and lone-pair directions, and the cylindrically symmetric quadrupole,  $Q_5$ , which, if it has a positive population, redistributes charge from the plane of the bonds into directions above and below the plane. For the hydrogens, the dipole,  $D_3$ , with a positive lobe in the direction of the bonded nitrogen and a negative lobe in the opposite direction, and the quadrupole,  $Q_5$ , oriented with positive lobes in the bonding and anti-bonding directions and negative lobe in the plane perpendicular

to this direction, are expected to be dominant. Analyses in which only these multipoles are included will be referred to as ' $\bar{6}m2$ ' refinements.

The site symmetry of the heavy atoms in the isolated molecule is  $mm2$ . Under this symmetry the dipole  $D_1$ , the quadrupole  $Q_1$  and the octupole  $O_5$  are allowed in addition to those of the  $\bar{6}m2$  site symmetry. Analyses including these terms will be referred to as ' $mm2$ ' refinements.

Analyses excluding all multipoles of non-zero order will be referred to as 'scalars only' refinements.

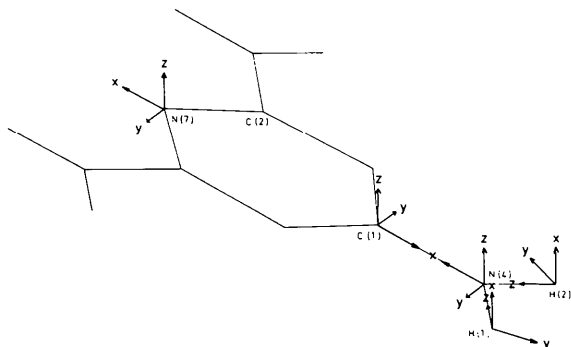


Fig. 2. The local coordinate systems for the atoms C(1), N(4), N(7), H(1) and H(2) (idealized). For details see text. The coordinate systems for the remaining atoms are similarly defined.

### Standard molecular exponents

Following the triazine and earlier analyses the initial model had the valence exponents,  $\zeta_i$ , for each atom, fixed at the standard molecular values of Hehre, Stewart & Pople (1969). A series of analyses were made including various multipole terms in the model. The results with the models of the 'scalars only' and ' $\bar{6}m2$ ' levels, but without the dipole or quadrupole functions on the hydrogens, are shown in Table 2.

The GoF parameter provides an appropriate statistical test for the adequacy of the model. Following the normal (but doubtful) practice, the least-squares parameter errors have been multiplied by the GoF. Parameter estimates are shown with the errors, as a fraction of the last significant figure, enclosed in parentheses.

For the standard molecular refinement of melamine the inclusion of the appropriate multipole terms in the charge-density model lowers the GoF from 4.80 (5) at the scalars-only level to 4.25 (5) with the inclusion of the  $\bar{6}m2$  multipoles. At the same time the  $R_w$  refinement index decreases from 0.049 to 0.042. Although this is a highly significant improvement in the fit to the experiment the high final value of the GoF suggests that the data contains far more information on the valence density.

In contrast to the results with refined exponents (see below), there is little evidence of trends systematic with the hydrogen-bonding scheme.

Table 2. Standard molecular exponents, 'scalars only' and  $\bar{6}m2$  site symmetry

Units are bohr<sup>-1</sup> for  $\zeta$ , e for the populations. The projection coefficient is referred to as proj. Each set of parameters for like atoms is followed by a mean. The number in parentheses refers to the standard deviation,  $S_{\sigma}$ , of the distribution of parameters. The mean parameter e.s.d.,  $\sigma$ , is given by the number in square brackets. Asterisks label those results where  $S_{\sigma} > 2\sigma$ .

Atom	Scalars only		$\bar{6}m2$ site symmetry			
	$\zeta$	$P_{\text{val}}$	$\zeta$	$P_{\text{val}}$	$Q_5$	$O_1$
H(1)		0.85 (2)		0.79 (2)		
H(2)		0.77 (2)		0.73 (2)		
H(3)	1.24	0.75 (2)	1.24	0.69 (2)		
H(4)		0.77 (2)		0.72 (2)		
H(5)		0.82 (2)		0.80 (2)		
H(6)		0.82 (2)		0.81 (2)		
		0.80 (4) [2]*		0.76 (5) [2]*		
C(1)		3.82 (3)		3.76 (2)	-0.139 (15)	0.007 (21)
C(2)	1.72	3.77 (2)	1.72	3.69 (2)	-0.158 (15)	0.055 (22)
C(3)		3.76 (2)		3.70 (3)	-0.142 (15)	0.031 (22)
		3.78 (3) [2]		3.72 (4) [2]	-0.146 (10) [15]	0.031 (24) [21]
Amine	N(4)	5.34 (2)	1.95	5.44 (2)	0.031 (15)	0.140 (21)
		5.28 (2)		5.38 (2)	-0.023 (15)	0.188 (21)
		5.31 (2)		5.38 (2)	-0.035 (15)	0.094 (21)
		5.31 (3) [2]		5.40 (3) [2]	-0.009 (35) [15]*	0.141 (47) [21]*
Ring	N(7)	5.39 (3)	1.95	5.44 (2)	0.077 (15)	0.139 (21)
		5.27 (2)		5.34 (2)	-0.146 (15)	0.140 (19)
		5.28 (2)		5.34 (2)	-0.034 (15)	0.122 (19)
		5.31 (7) [2]*		5.37 (6) [2]*	-0.035 (112) [15]*	0.134 (10) [20]
$R = 0.085$		$R_w = 0.049$	$R = 0.077$		$R_w = 0.042$	
GoF = 4.80 (5) Proj. = 1.08			GoF = 4.25 (5) Proj. = 1.04			

### Optimized exponents

The X-ray data was again analysed in terms of the valence-density model, but with the radial exponents of the monopole terms optimized by the method discussed by Price, Maslen & Delaney (1978). For each atom type, the exponents of the higher-order terms were fixed at values close to the mean (optimized) monopole exponents. Thus the H dipoles and quadrupoles had exponents of  $1.3 \text{ bohr}^{-1}$ , while the C multipoles had exponents of  $1.67 \text{ bohr}^{-1}$ , those of the amine N atoms were  $1.88 \text{ bohr}^{-1}$  and those of the ring N atoms were  $1.85 \text{ bohr}^{-1}$ .

A number of analyses were made which included different multipole terms. It was immediately apparent that the fit of the model to the data was dramatically improved by the optimization of both the monopole exponent and the population of the trigonal (bond-directed) octupole term ( $O_1$ ). Addition of further terms tended to result in less significant improvements. As the number of parameters increased, the correlation between certain terms did likewise. A consequence is that the parameters become increasingly model-dependent.

Only the results of those analyses where the multipoles were those of the three previously defined approximation schemes are reported in detail. The results are given in Tables 3 and 4.

The inclusion of the exponent as a parameter has resulted in a large improvement in the model, the GoF parameter falling more than  $30\sigma$  from 4.95 (5) to

3.40 (5). At the same time, the  $R_w$  index decreases from 0.049 to 0.035. This is a highly significant improvement.

The exponents are surprisingly well determined. There is good agreement between charge-density parameters within each group of like atoms, and the agreement between the C atoms, which are isolated from hydrogen bonding and other intermolecular forces, is particularly close. Within each group there is an inverse correlation between the population of the monopole term and its exponent. This suggests that the difference in the electron density between like atoms is relatively small in regions near where the density function is a maximum.

The final values of the exponents are quite different from, and usually less than, the standard molecular values. The mean carbon value of 1.680 (5)\* is the

\* For the means of parameters, here and in the tables, the number enclosed in parentheses is the estimated width (standard deviation),  $S_x$ ,

$$S_x = [\Sigma(x - \bar{x})^2 / (n - 1)]^{1/2}$$

of the distribution of parameters, rather than the estimated standard error of the mean. The latter is smaller by a factor of  $n^{1/2}$ , where  $n$  is the number of parameters in the sample. As before, the notation is such that the width is in units of the last figure quoted of the mean. In the tables the number enclosed in square brackets is the mean parameter e.s.d.,  $\bar{\sigma}$ . If  $S_x$  is substantially greater than  $\bar{\sigma}$  then the parameters are unlikely to all belong to the same parent population. In other words, this is evidence of systematic differences between the parameters.

Table 3. Optimized exponents, 'scalars only' and ' $\bar{6}m2$ ' site symmetry

Notation and units as for Table 2.

Atom	Scalars only		$\bar{6}m2$ site symmetry				
	$\zeta$	$P_{\text{val}}$	$\zeta$	$P_{\text{val}}$	$D_3$	$Q_5$	$O_1$
H(1)	1.130 (49)	0.880 (36)	1.147 (32)	0.788 (31)	0.091 (11)	0.077 (16)	
H(2)	1.226 (51)	0.767 (37)	1.260 (37)	0.659 (30)	0.074 (11)	0.034 (16)	
H(3)	1.513 (53)	0.629 (38)	1.454 (41)	0.665 (32)	0.151 (12)	0.055 (16)	
H(4)	1.253 (51)	0.795 (37)	1.236 (37)	0.755 (31)	0.158 (11)	0.063 (16)	
H(5)	1.461 (53)	0.698 (38)	1.292 (35)	0.853 (27)	0.168 (11)	0.055 (15)	
H(6)	1.180 (49)	0.874 (36)	1.045 (36)	1.128 (29)	0.188 (10)	0.045 (15)	
	1.294 (156) [51]*	0.774 (99) [37]*	1.239 (138) [37]*	0.808 (173) [30]*	0.138 (45) [11]*	0.055 (15) [16]	
C(1)	1.674 (10)	3.569 (36)	1.602 (7)	3.792 (32)		-0.161 (10)	0.146 (14)
C(2)	1.683 (10)	3.516 (34)	1.610 (7)	3.807 (33)		-0.184 (10)	0.110 (14)
C(3)	1.683 (10)	3.531 (35)	1.620 (7)	3.761 (32)		-0.157 (10)	0.126 (13)
	1.680 (5) [10]	3.539 (27) [35]	1.610 (9) [7]	3.787 (23) [32]		-0.167 (15) [10]	0.127 (18) [14]
Amine	N(4)	1.869 (8)	5.451 (39)	1.867 (9)	5.415 (52)	-0.015 (11)	0.249 (13)
	N(5)	1.885 (8)	5.377 (37)	1.915 (9)	5.073 (52)	-0.005 (11)	0.164 (14)
	N(6)	1.871 (8)	5.421 (38)	1.941 (9)	4.902 (46)	0.020 (10)	0.139 (14)
		1.875 (9) [8]	5.416 (37) [38]	1.908 (38) [9]*	5.130 (261) [50]*	0.000 (18) [11]	0.184 (58) [14]*
Ring	N(7)	1.854 (7)	5.424 (30)	1.879 (7)	5.389 (29)	-0.093 (9)	0.165 (12)
	N(8)	1.831 (7)	5.573 (32)	1.832 (8)	5.557 (29)	-0.074 (9)	0.200 (12)
	N(9)	1.836 (7)	5.494 (31)	1.844 (8)	5.456 (30)	-0.080 (10)	0.172 (12)
		1.840 (12) [7]	5.497 (75) [31]*	1.848 (19) [8]*	5.467 (85) [29]*	-0.082 (10) [9]	0.179 (19) [12]

$R = 0.057$   $R_w = 0.035$   
GoF = 3.40 (5) Proj. = 1.05 (1)

$R = 0.0469$   $R_w = 0.0241$   
GoF = 2.33 (3) Proj. = 0.988 (12)

Table 4. *Optimized exponents, 'mm2' site symmetry*

Notation and units as for Table 2.

Atom	$\zeta$	$P_{\text{val}}$	$D_3/D_1$	$Q_1$	$Q_5$	$O_1$	$O_5$	
H(1)	1.066 (44)	0.984 (48)	0.188 (20)		0.147 (20)			
H(2)	1.134 (44)	0.908 (48)	0.158 (20)		0.113 (20)			
H(3)	1.430 (45)	0.662 (46)	0.152 (19)		0.061 (20)			
H(4)	1.177 (42)	0.813 (47)	0.165 (20)		0.071 (20)			
H(5)	1.537 (45)	0.610 (46)	0.061 (15)		-0.032 (17)			
H(6)	1.156 (43)	0.849 (47)	0.097 (15)		-0.012 (17)			
	1.250 (188) [44]*	0.804 (144) [47]*	0.137 (48) [18]*		0.058 (69) [19]*			
C(1)	1.573 (8)	4.108 (47)	0.004 (12)	0.025 (12)	-0.221 (12)	0.238 (17)	0.003 (13)	
C(2)	1.578 (8)	4.120 (47)	-0.084 (12)	0.012 (12)	-0.249 (12)	0.211 (17)	-0.034 (13)	
C(3)	1.570 (8)	4.141 (47)	-0.019 (11)	0.022 (12)	-0.236 (11)	0.267 (17)	-0.071 (13)	
	1.574 (4) [8]	4.123 (16) [47]	-0.033 (46) [12]*	0.020 (7) [12]	-0.235 (14) [12]	0.239 (28) [17]	-0.034 (37) [13]*	
Amine	N(4)	1.915 (10)	4.864 (89)	0.036 (14)	-0.015 (12)	0.057 (15)	0.179 (17)	0.020 (13)
	N(5)	1.924 (10)	4.957 (90)	-0.008 (14)	-0.038 (12)	0.003 (15)	0.179 (17)	0.040 (13)
	N(6)	1.903 (10)	5.255 (91)	-0.158 (12)	-0.065 (11)	0.009 (11)	0.142 (17)	0.017 (13)
		1.914 (10) [10]	5.025 (205) [90]*	-0.043 (102) [13]*	-0.039 (25) [12]*	0.023 (30) [14]*	0.167 (21) [17]	0.026 (13) [13]
Ring	N(7)	1.901 (6)	5.134 (37)	0.102 (8)	0.062 (9)	-0.060 (10)	0.117 (13)	0.030 (11)
	N(8)	1.855 (6)	5.350 (39)	0.059 (8)	0.037 (9)	-0.048 (10)	0.151 (13)	0.011 (11)
	N(9)	1.869 (6)	5.245 (38)	0.067 (8)	0.044 (9)	-0.039 (10)	0.118 (13)	0.040 (11)
		1.875 (24) [6]*	5.243 (108) [38]*	0.076 (23) [8]*	0.048 (13) [9]	-0.049 (11) [10]	0.129 (19) [13]	0.027 (15) [11]
$R = 0.0447$		$R_w = 0.0240$		$\text{GoF} = 2.33 (3)$		$\text{Proj.} = 0.985 (15)$		

same as, but much better defined than those obtained at the same level of refinement in the diamond and triazine analyses. The mean value of the exponent for the amine nitrogens is 1.875 (9) and this is somewhat greater than the mean value of 1.840 (12) for the ring nitrogens. In the triazine analysis the nitrogen exponent at this level of the model was 1.83 (4). The hydrogen exponents vary considerably and the mean value is 1.29 (16), which is the same as obtained in the triazine analysis.

Comparison of Tables 2, 3, and 4 shows that the populations change, with exponent refinement, in such a way as to accentuate the charge alternation. At the 'scalars only' level the mean carbon valence population decreases from 3.78 (3) to 3.54 (3). The latter value agrees with the INDO gross Mulliken of Table 1, but not with the CNDO/2 or STO-3G standard molecular (SM) values. The mean amine nitrogen population increases from 5.31 (3) to 5.42 (4) while for the ring nitrogens the increase is from 5.31 (7) to 5.50 (7). It is interesting that the standard molecular analysis is unable to detect differences between these two types of nitrogen. The mean hydrogen population does not change significantly [from 0.80 (4) to 0.77 (10) e] but the distribution of values broadens appreciably.

#### Multipoles of $\bar{6}m2$ symmetry

The GoF index at the  $\bar{6}m2$  level, with the 'bond-directed' multipoles  $Q_5$  and  $O_1$  on the heavy atoms, and  $D_3$  and  $Q_5$  on the hydrogen atoms, is 2.33 (3), some 25 to 30 $\sigma$  less than the 'scalars only' result. The final  $R_w$  index falls to 0.0241. This model has just 61

parameters. With standard molecular exponents and the same multipole density terms, the result was a GoF of 4.25 (5) and an  $R_w$  index of 0.042, some 50 $\sigma$  worse in the fit of the model to the data.

As at the 'scalars only' level, the exponents are well-determined and comparable within each group of like atoms. The carbon atom exponents are the same within the errors, with a mean value of 1.610 (9) bohr<sup>-1</sup>. This is a marked change from the exponents with scalar terms alone. The nitrogen atom exponents and the hydrogen atom exponents (and populations) are not the same within the errors. The amine nitrogen exponents have a mean of 1.91 (4) bohr<sup>-1</sup> while that of the ring nitrogen exponents is 1.85 (2) bohr<sup>-1</sup>. The mean hydrogen exponent is 1.24 (14) bohr<sup>-1</sup>.

The spread of values within each group has increased a little. The mean carbon population increased from 3.54 (3) to 3.79 (2) e. That of the amine nitrogens decreases from 5.42 (4) to 5.13 (26) and that of the ring nitrogens from 5.50 (7) to 5.47 (8) e. The mean hydrogen population changes little from 0.77 (10) to 0.81 (17) e.

Many of the angular distortion terms are highly significant. On the heavy atoms, the trigonal octupole  $O_1$  is directed with its positive lobes (as nearly as possible to) lying along the bonding directions. In contrast to the results with standard molecular exponents the present  $O_1$  populations are all large and positive. They have comparable values for the nitrogen atoms, the mean population being 0.18 e (0.6 e per lobe) which is ca 13 $\bar{\sigma}$ . The values for the carbon atoms are smaller but comparable, with a mean population of 0.13 e (0.04 e per lobe) which is 9 $\bar{\sigma}$ . There are

highly significant  $Q_5$  populations on the carbons and on the ring nitrogens, but not on the amine nitrogens. The negative value for these populations is a measure of electron transfer from above and below the plane of the ring into that plane. These quadrupole populations are comparable within each group of like atoms, but the values for the carbon atoms (a mean of 0.17 e shifted into the plane of the ring) are about twice those for the ring nitrogens. The significance of the terms is such that the populations are some  $17\sigma$  on the carbon atoms and some  $9\sigma$  on the ring nitrogens.

Even on the hydrogen atoms the populations of the bond-directed multipole terms ( $D_3$  and  $Q_3$ ) are highly significant. All the populations are of such a sign as to redistribute electrons into the bonding directions from the antibonding directions ( $D_3$ ) and from the plane perpendicular to the bonding directions ( $Q_3$ ). The dipole populations vary in magnitude from 0.07 to 0.17 e (7 to  $18\sigma$ ). The quadrupole populations are not as significant, ranging from 0.03 to 0.08 e (2 to  $5\sigma$ ).

When the heavy-atom site symmetry is relaxed to  $mm2$  the extra allowed multipoles are the dipole  $D_1$ , the quadrupole  $Q_1$ , and the octupole  $O_3$ . The GoF with the inclusion of these terms is 2.33 (3) which is not significantly different from the  $\bar{6}m2$  analysis. Neither is there any reduction in the  $R_w$  index, which has a value of 0.0240. There are 88 parameters in the model, an increase of 27 over the  $\bar{6}m2$  level. The  $\bar{6}m2$  analysis is thus a much more efficient description of the charge density, as it results in just as good a fit to the data with many less parameters. It is sometimes believed that if the addition of some parameters to a least-squares model does not result in a significant decrease in the GoF then the estimated values of the added parameters will not be significantly different from zero, and neither will there be any significant changes in the estimates of the other parameters. Because of correlation this is not generally the case and in the present situation the estimated valence populations, for example, are many  $\sigma$  different for the two models.

Once again the exponents are well-defined and comparable within each group of like atoms. The increased number of parameters results in an increased width in the distribution of parameters within each group. The mean carbon exponent decreases to 1.574 (4) bohr<sup>-1</sup>. There is little change in the nitrogen or hydrogen exponents, the mean values being 1.91 (1) for the amine nitrogens, 1.88 (2) for the ring nitrogens and 1.25 (19) bohr<sup>-1</sup> for the hydrogens.

The carbon valence populations are quite different from the  $\bar{6}m2$  results, the 'charge alternation' of the structure being markedly reduced in this model.

The addition of the extra dipole, quadrupole and octupole terms to the model results in a reduction of the significance of the other angular functions while some of the new terms have significant populations. The dipole on atom C(2) is some  $7\sigma$  and (assuming the

accuracy of the neutron positional parameters) indicates that the charge transfer is greater into the bonds of the ring than into the bond to the amine nitrogen. The large (0.16 electrons or  $13\sigma$ ) negative dipole term on atom N(6) seems to indicate a transfer of charge from the C–N bond to the N–H bonds to H(5) and H(6). As expected, the correlation between this dipole population and those of the adjacent hydrogens [H(5) and H(6)] is fairly large ( $\sim 0.5$ ) and this results in much less significant ( $4\sigma$  and  $6\sigma$  respectively) dipoles on H(5) and H(6). This amine group is the least planar of the three and consequently the description of the charge density is expected to be less accurate. In addition it was noticed in many analyses that the charge separation between the atoms N(6) and H(6) was sensitive to the coefficient  $r^*$  in the extinction correction. The reflections most affected by extinction have their reciprocal-lattice vectors almost normal to the plane. The problem with extinction is presumably related to the fact that H(6) is the atom which deviates most from this plane.

There are large ( $13\sigma$ ,  $7\sigma$  and  $8\sigma$ ) positive dipoles on the ring nitrogens, showing that the lone-pair direction has (0.06 to 0.10) more electrons than the two bonding directions.

A positive population for the  $Q_1$  quadrupole terms shows a redistribution of electrons from the  $yz$  plane to the  $xz$  plane, the effect being maximal in the plane  $z = 0$ . There are consistent but small positive terms on the carbon atoms which are difficult to understand. It must be remembered, however, that random errors in the neutron positional parameters would be expected to result in random non-zero dipole populations, and random errors in the neutron thermal parameters would likewise produce additional random bias in the quadrupole terms. The  $Q_1$  quadrupole populations are somewhat larger and negative on the amine nitrogens, and positive on the ring nitrogens. The latter may be a result of the bond angle being a little less than  $120^\circ$  at the ring nitrogens.

The magnitude of the  $\bar{6}m2$ -allowed  $Q_5$  quadrupole increases by 0.07 e on the carbon atoms, but remains barely significant on the amine nitrogens. The mean magnitude of the terms on the ring nitrogens decreases by 0.03 e. Similarly, the populations of the bond-directed octupole,  $O_1$ , remain positive and highly significant on all the heavy atoms. The populations of the  $\bar{6}m2$ -forbidden heavy-atom  $O_5$  octupoles are small ( $\leq 0.07$  e). They are [with the exception of C(1)] negative on the carbon atoms and positive on the nitrogens.

#### Inclusion of bond-directed multipoles of high exponent

In an attempt to explore the radial dependence of the principal multipole terms of non-zero order, various analyses were made with the inclusion of terms of high

Table 5. *Optimized scalar exponents, inclusion of bond-directed sharp multipoles*

Notation and units as for Tables 2, 3 and 4.

Atom	$\zeta$	$P_{\text{val}}$	C, N $O_{1A}$ H $D_{3A}$	C, N $O_{1B}$ H $D_{3B}$	H $Q_{5A}$	H $Q_{5B}$	Exponents
H(1)	1.102 (41)	0.801 (33)	0.019 (16)	0.042 (26)	0.014 (20)	0.002 (77)	$A = 2 \text{ bohr}^{-1}$
H(2)	1.240 (42)	0.648 (34)	0.003 (17)	0.043 (23)	0.004 (20)	-0.041 (86)	
H(3)	1.447 (44)	0.637 (35)	0.058 (18)	0.005 (30)	0.019 (21)	-0.084 (89)	
H(4)	1.225 (42)	0.734 (33)	0.051 (16)	0.055 (26)	-0.006 (20)	-0.048 (76)	
H(5)	1.276 (43)	0.839 (32)	0.082 (16)	0.007 (27)	-0.001 (20)	0.034 (82)	
H(6)	1.050 (40)	1.108 (31)	0.123 (16)	-0.040 (27)	0.016 (13)	-0.001 (42)	
	1.223 (140) [42]*	0.794 (173) [33]*	0.056 (43) [17]*	0.019 (35) [27]	0.008 (10) [19]	-0.023 (42) [75]	
C(1)	1.635 (8)	3.606 (34)	0.050 (19)	0.108 (39)			$A = 2 \text{ bohr}^{-1}$
C(2)	1.647 (8)	3.609 (34)	0.001 (20)	0.219 (39)			
C(3)	1.635 (8)	3.647 (34)	0.047 (19)	0.127 (38)			
	1.639 (7) [8]	3.621 (23) [34]	0.033 (27) [19]	0.151 (59) [39]			
Amine	N(4)	1.856 (7)	5.540 (45)	0.261 (23)	-0.082 (48)		$B = 6 \text{ bohr}^{-1}$
	N(5)	1.897 (7)	5.308 (45)	0.117 (24)	0.117 (50)		
	N(6)	1.925 (7)	5.035 (45)	0.104 (23)	0.059 (48)		
		1.893 (35) [7]*	5.295 (253) [45]*	0.161 (87) [23]*	0.031 (102) [49]*		
Ring	N(7)	1.868 (5)	5.409 (28)	0.150 (18)	0.021 (40)		
	N(8)	1.832 (5)	5.562 (28)	0.193 (18)	-0.032 (40)		
	N(9)	1.834 (5)	5.518 (28)	0.132 (18)	0.073 (40)		
		1.844 (20) [5]*	5.496 (79) [28]*	0.158 (31) [18]	0.021 (53) [40]		
$R = 0.0501$		$R_w = 0.0277$		$\text{GoF} = 2.685 (4)$		$\text{Proj.} = 1.023 (12)$	

exponent. The terms included were the bond-directed multipoles  $O_1$  on the heavy atoms, and  $D_3$  and  $Q_5$  on the hydrogens. The results are shown in Table 5. The 'diffuse' multipoles had exponents,  $\zeta$ , fixed at  $2 \text{ bohr}^{-1}$  and the 'sharp' multipoles had exponents of  $6 \text{ bohr}^{-1}$  for the hydrogen dipole and quadrupole. The radial density functions are of the usual form  $Nr^n e^{-2\zeta r}$ , where  $N$  is the normalization factor.

The high correlation between the terms increases the e.s.d.'s substantially. On the carbon atoms, the populations of the diffuse octupole terms, while being positive, are barely significant. The sharp octupole terms, on the other hand, have positive populations of 0.1 to 0.2 e ( $3-5\sigma$ ). On the nitrogen atoms, the position is reversed. The diffuse octupoles on all the nitrogens have consistently positive and significant populations (of 0.10 to 0.26 e), describing, as before, the charge movement into the chemical bonds. With two exceptions, the populations of the sharp octupoles on the nitrogens are also positive. The exceptions are the amine nitrogen N(4) and the ring nitrogen N(8), which have small negative populations.

Apart from the sharp dipole on H(6), all the dipole terms on the hydrogen atoms have positive populations. There is a (relatively) large negative sharp dipole on H(6) which is consistent with the neutron bond length being too small. This atom has the largest diffuse dipole population. Of the other diffuse terms, those on H(3) and H(5) are the largest. The reverse situation is true of the sharp dipole terms. Those on H(3) and H(5) are negligible, while those on H(1), H(2) and H(4) are

positive and comparable in size. None of the quadrupole terms on the hydrogen atoms have significant populations.

### The convolution approximation

The existence of the positive populations for the sharp dipole term on hydrogen atoms H(1), H(2) and H(4) is puzzling. Difference density maps from theoretical calculations indicate that the distortion in the density due to bonding in the vicinity of the hydrogen atoms can be well-represented by diffuse terms. Sharp terms would be expected if there were errors in the neutron bond lengths, and these errors would need to be in such a direction as to consistently overestimate the lengths of the bonds to the atoms H(1), H(2) and H(4).

Table 6 lists the population of the sharp dipole terms for the hydrogen atoms together with certain geometrical features including the neutron and X-ray N-H bond-lengths, the difference between these (N-X distances), and the difference amplitudes of vibration for these atoms. The latter were estimated by assuming that the thermal motion of a hydrogen atom consists of a rigid-body riding motion of the hydrogen on its bonded nitrogen nearest neighbour, together with an additional, uncorrelated motion. An 'internal modes' thermal-motion tensor was obtained by subtracting the U tensor of the bonded N atom from that of the H atom. The principal axes of these difference ellipsoids were approximately aligned with the



Table 6. *Correlation of sharp hydrogen dipole populations with geometrical features*

The H atoms are in order of increasing hydrogen-bond strength, apart from H(6). The difference-amplitude tensor was obtained by subtracting the mean-square-amplitude vibration tensor for each amine nitrogen from that of the corresponding hydrogen atoms. The principal axes of the difference ellipsoids correspond approximately to the local H atom coordinate system defined in the text. 'Bond' refers to the *z* component, '⊥' to the *x* component and '∥' to the *y* component. Distances are in Å, and dipole populations in e.

Atom	H-bond length	Sharp dipole	R.m.s. difference amplitudes Bond	Plane		Covalent bond lengths		
				⊥	∥	<i>N</i>	<i>X</i>	<i>N-X</i>
H(3)	—	0.01	0.05	0.27	0.16	1.002	0.91	0.09
H(5)	—	0.01	0.06	0.21	0.16	1.000	0.93	0.07
H(6)	2.08	-0.04	0.08	0.18	0.13	1.021	0.93	0.09
H(2)	2.11	0.04	0.09	0.13	0.15	1.009	0.88	0.12
H(1)	2.05	0.04	0.07	0.15	0.12	1.027	0.81	0.22
H(4)	2.00	0.05	0.09	0.12	0.13	1.024	0.88	0.14

local H atom coordinate systems. The difference tensors were expressed in terms of these coordinates, and the square roots of the diagonal elements taken as representing the r.m.s. internal-motion amplitudes. The first term is a bond-stretching motion (in the *z* direction), the second is approximately perpendicular to the plane of the amine group (in the *x* direction) and the third is approximately in this plane (the *y* direction). The hydrogen atoms in the table are collected into three groups. Firstly, atoms H(3) and H(5) are not hydrogen-bonded. Atom H(6) is listed separately. As discussed earlier, this atom has two close intermolecular contacts in addition to the hydrogen bond. This close packing results in a large deviation in the atom's position from the plane of the amine group. This appeared to be connected to the strong correlation of the H(6) population with the extinction coefficient. As a result, less confidence was attached to the H(6) parameters generally. Atoms H(1), H(2) and H(4) are hydrogen bonded.

Table 6 shows correlation between the size of the bond-stretching vibration amplitude and the size of the sharp dipole term. The exception is H(6), which has a negative sharp dipole population of 0.04 e. Effects which might produce the correlations evident in Table 6 are a hydrogen-bond-correlated systematic error in the neutron coordinates, anharmonic thermal motion and the use of the convolution approximation to describe the thermal motion. The first of these seems rather unlikely. Anharmonic contributions could be considered as a sum of two contributions, namely an anharmonic, principally third-order, bond-stretching and the effect of libration of the hydrogen atom about the nitrogen (or carbon) atom.

The effect of the bond-stretching anharmonic thermal motion is the same for the neutron and X-ray data. There were no anharmonic terms included in the neutron analysis and thus the neutron positions quoted are mean positions and not the equilibrium positions. The anharmonic motion would be in such a direction as to make the mean bond length greater than the

equilibrium bond length. If an anharmonic correction had been applied in the neutron analysis but not in the X-ray analysis, then the use of the equilibrium bond length instead of the mean bond length would result in an apparent shift in the centroid of the hydrogen atom charge density away from the nitrogen atom. This would show up in sharp dipole terms directed outward from the nitrogen atom. The dipole terms detected here are in the opposite direction.

If the thermal motion of the hydrogen atom is principally one of libration about the nitrogen atom then the apparent bond length is less than the true bond length. This bond shortening is proportional to the bond length and to the amplitude of libration. As the centroid of the hydrogen atom charge density is between the hydrogen nucleus and the nitrogen nucleus, the bond shortening is greater for the neutron data than for the X-ray data. The net effect is that the hydrogen atom charge density will appear to be a little further from the nitrogen atom. The size of this effect would be proportional to the amplitude of vibration of the hydrogen atom perpendicular to the bond. The effect detected here is opposite in sign to this, and also oppositely correlated with this amplitude of vibration.

The convolution approximation makes the assumption that each density function rigidly follows the motion of the nucleus on which it is centred. As indicated by Stewart (1974), this assumption has dubious validity, but nonetheless forms the basis of a working approximation for both structural and charge-density analysis of X-ray diffraction data.

The effect of thermal motion on the charge density of a molecule is well described in the Born-Oppenheimer approximation, which requires that the molecular charge density be recalculated for each configuration of the nuclei. This allows for the deformation of the pseudo-atoms as they vibrate whereas the convolution approximation does not.

There has been little work done on investigating the adequacy of the convolution approximation for the analysis of accurate X-ray diffraction data. The extent

of the deformation of a pseudo-atom will obviously depend on its definition, *i.e.* on how the molecular density is partitioned. The meaning of such a partitioning is especially unclear in regions equidistant from two or more nuclei. Fortunately, the electron density in this region is rather low, and is only marginally affected by thermal motion, and this problem can be neglected for most purposes. However, the electron density near the nucleus is also affected by a change in the internuclear separation. Coulson & Thomas (1971) studied the effect for  $H_2^+$  and  $H_2$ , and although their definition of a pseudo-atom is not clear, they conclude that 'a full Born–Oppenheimer study of the changes in the charge cloud during vibration leads to bond contraction in the ground vibrational state of  $H_2^+$  which is about 0.124 bohr instead of a convolution-model contraction of 0.096 bohr'. In Fig. 3, which is a reproduction of Coulson & Thomas's (1971) Fig. 2, the effect of thermal motion, in both the Born–Oppenheimer approximation and the convolution approximation, on the axial charge density near the hydrogen nucleus in  $H_2^+$ , is shown. The difference between the Born–Oppenheimer and convolution-approximation dynamic densities is largest near the nuclear position. It is positive in the region between the nuclei and negative in the opposite direction. If this inaccuracy in the treatment of thermal motion was parameterized in terms of the functions of Stewart's charge-density model, then it would result primarily in a small, sharp dipole term directed into the bond. The

difference between the two approximations would be expected to increase with the amplitude of thermal vibration, and hence the size of such a sharp dipole term would be correlated with the amplitude of the bond-stretching thermal vibration.

To what extent the results of Coulson & Thomas (1971) for  $H_2$  and  $H_2^+$  are transferable to molecules such as melamine, or even to diatomic hydrides, is, as yet, unknown. However, the effect is expected to be similar in size and direction. The results of Becker (1975) on BeH support this. Epstein & Stewart (1975) have recently studied the deformation of the pseudo-atom densities with vibration for BH. Their preliminary results indicated that the pseudo-atoms do, indeed, deform substantially.

The inadequacy of the convolution approximation to describe the change in the molecular charge density with thermal smearing would seem, therefore, to be the one effect which can explain the existence of the sharp dipole terms, directed into the NH bond, and correlated with the amplitude of bond-stretching internal vibrations.

### The effect of hydrogen bonding

As noted above, the population parameters within each group of like atoms are in good agreement. The differences however, while being small in comparison to those between unlike atoms, are in many cases larger than the e.s.d.'s. In Tables 2 to 5 asterisks appended to means denote those cases where the differences  $S_x$  exceed  $2\sigma$ .

Before investigating the correlation between hydrogen bonding and *selected* population parameters it is necessary to show that the correlation is not unique to those few sets selected for closer study. For example, parameters for N(8) may be randomly different from those of N(7) and N(9) and thus a certain fraction of the sets of parameters where  $S_x > \bar{\sigma}$  would be expected to 'correlate with hydrogen bonding' in this way by chance alone. An indication of whether the correlation is coincidental or not is given by the fraction of cases when  $S_x \geq 2\bar{\sigma}$  (or  $\bar{\sigma}$ ) which can be correlated with hydrogen bonding. If this fraction is of the order of 0.5 or more then the likelihood of the correlation being coincidental is small. On the other hand, if it is less than 0.5 the correlation of selected sets of parameters with hydrogen bonding must be viewed with suspicion.

These fractions, for the seven analyses whose results are displayed in Tables 2 to 5, are shown in Table 7. The criteria for correlation are as follows. (i) For the hydrogen atoms the parameters for H(3) and H(5) were required to be greater or less than those of H(1), H(2) and H(4). (ii) Any cases of  $S_x \geq 2\bar{\sigma}$  (or  $\bar{\sigma}$ ) for the parameters of the carbon atoms were taken as not correlated with hydrogen bonding. (iii) For the amine nitrogens the N(4) populations were required to be

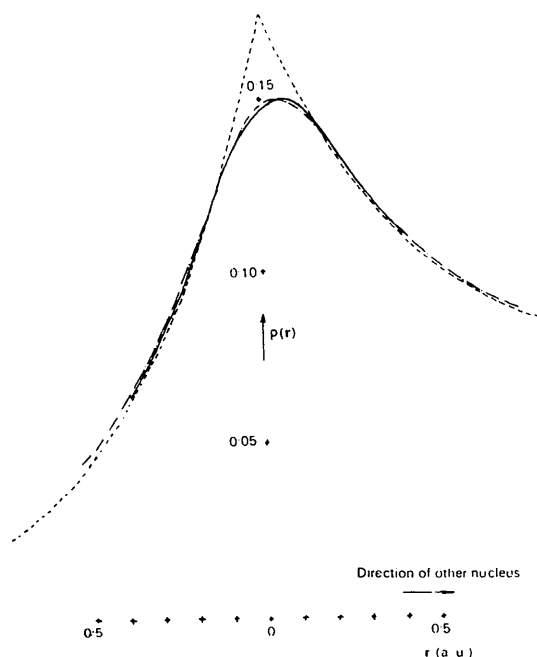


Fig. 3. Axial charge density for  $H_2^+$ . Dashed line: static density when  $R = R_e$ ; solid line: dynamic density (Born–Oppenheimer approximation); chain-dotted line: dynamic density (convolution approximation). Results taken directly from Coulson & Thomas (1971).

Table 7. Evidence that the systematic differences are correlated with the hydrogen-bonding scheme

For a particular analysis the variation ( $S_x$ ) within the parameters of a set was larger than twice the mean parameter e.s.d. ( $\bar{\sigma}$ ) for  $p$  parameter sets and larger than  $\bar{\sigma}$  for  $q$  parameter sets. Only some ( $n$  and  $m$  respectively) of these systematic differences could reasonably be correlated with hydrogen bonding. The fractions  $n/p$  and  $m/q$  are shown below. Fractions greater than 0.5 indicate a small likelihood that the correlations are coincidental.

	$s_x > 2\bar{\sigma}$	$s_x > \bar{\sigma}$
Analyses with standard molecular exponents		
Scalars only	0/2	0/4
$\bar{6}m2$ symmetry	2/5	3/8
Analyses with optimized exponents		
Scalars only	3/3	3/5
$\bar{6}m2$ symmetry	7/8	10/14
$mm2$ symmetry	9/13	11/20
Sharp multipoles	6/9	9/14

different from those of N(5) and N(6). (iv) For the ring nitrogens the N(8) parameters were required to be different from those of N(7) and N(9), while the latter were required to be similar.

The first column of Table 7 shows the relevant fractions for these sets of parameters where  $S_x \geq 2\bar{\sigma}$ , and the second those when  $S_x > \bar{\sigma}$ .

For the analyses with standard molecular exponents, all of these fractions are less than 0.5. Identification of systematic differences within a parameter set with hydrogen-bonding effects from these analyses alone is dubious. However, in all the analyses with optimized exponents, the fractions are greater than 0.5. The strongest evidence that the systematic differences are due to hydrogen bonding comes from the analyses with refined exponents at the 'scalars only' and  $\bar{6}m2$  levels, where the correlation coefficients in the least-squares are reasonably small. In the former analysis all three of the cases where  $S_x \geq 2\bar{\sigma}$  can be correlated with hydrogen-bonding, and in the latter analysis seven of the eight such cases can be correlated.

In analyses with optimized exponents at the  $\bar{6}m2$  and  $mm2$  symmetry levels only the carbon atom valence populations show no systematic differences. These atoms are well-shielded from intermolecular forces by the neighbouring atoms.

Table 8 shows some of the results from the analysis with optimized exponents at the  $\bar{6}m2$  level with the atoms arranged in sub-groups according to the hydrogen-bonding scheme. The hydrogen atoms are arranged as in Table 6, the ring nitrogens are arranged with N(8), the acceptor atom for two hydrogen-bonds, last, and the amine nitrogens are arranged with N(4), the donor atom for two hydrogen bonds, last. The other four nitrogen atoms participate in one hydrogen bond each. The carbon atoms do not participate directly in any hydrogen-bonds.

Amongst the hydrogens, while there is no trend in

Table 8. Correlation of results from the ' $\bar{6}m2$ ' analysis with hydrogen bonding

The atoms are in order of increasing hydrogen-bond strength. H atoms in the same order as Table 7. Ring N atoms are hydrogen-bond acceptors, H(8) is acceptor for two hydrogen bonds. Amine N atoms are donors, H(4) is donor atom for two hydrogen bonds.  $P\zeta^3$  is proportional (for like atoms) to the maximum amplitude (density) of the monopole term. For the unbonded atoms these numbers are 1.0 (H), 14.2 (C), and 33.8 (N). The experimental values for the carbon atoms are 0.16. The N values are not correlated with hydrogen bonding.

Atom	$\zeta$	$P_{\text{val}}$	$P\zeta^3$	$D_3$	$Q_5$	$O_1$
H(3)	1.45	0.66	2.0	0.15	0.05*	
H(5)	1.29	0.85	1.8	0.17	0.05	
H(6)	1.04	1.13	1.3	0.19	0.04	
H(2)	1.26	0.66	1.3	0.07	0.03	
H(1)	1.15	0.79	1.2	0.09	0.08	
H(4)	1.24	0.85	1.4	0.16	0.06	
N(7)	1.87	5.39	35.0		-0.09	0.17
N(9)	1.84	5.46	34.0		-0.08	0.17
N(8)	1.83	5.56	34.0		-0.07	0.20
N(6)	1.94	4.90	36.0		0.02	0.14
N(5)	1.92	5.07	36.0		0.00	0.16
N(4)	1.87	5.41	35.0		-0.01	0.25

\* The distribution width ( $S$ )  $< 1.5\bar{\sigma}$ , where  $\bar{\sigma}$  is the mean parameter e.s.d. In this case there is no statistical evidence for non-random differences within the parameters. Only the hydrogen quadrupoles are in this category.

the valence populations themselves (unlike the 'scalars only' and  $mm2$  analyses), the valence exponents of H(3) and H(5) are larger than those of H(2), H(1) and H(4). The parameter  $P\zeta^3$  is proportional to the charge density in the hydrogen valence density function in the vicinity of the nucleus. This is larger for H(3) and H(5) than for H(2), H(1) and H(4). With the exception of H(4), the magnitude of the diffuse dipoles are greater for the non-hydrogen-bonded hydrogen atoms, and with the exception of H(2), the magnitudes of the quadrupole terms are less for these atoms.

Amongst the ring nitrogens, the doubly hydrogen-bonded N(8) has the largest valence population and smallest valence exponent. It also has the largest octupole term. The latter is a quantitative measure of the type of effect noticed by Delbaere & James (1973), where, in a  $X-X$  (high angle) difference density map of 2,2'-anhydro-1- $\beta$ -D-arabino-furanosyl uracil they saw a polarizing effect of the hydrogen bond on the lone-pair density of the acceptor nitrogen. In the analysis with sharp ( $\zeta = 6$ ) octupoles on the heavy atoms (Table 5), it is interesting to see that the population of this term on N(8) is negative, whereas it is positive on N(7) and N(9). This would seem to indicate that the N(8) octupole term, in addition to being the largest, is somewhat more diffuse than those of N(7) and N(9).

The situation amongst the amine nitrogens is

complicated by the fact that the amine group of N(6) is strongly distorted from planarity. Thus the octupole term on N(6) is somewhat smaller. Once again, the nitrogen atom participating in two hydrogen bonds, N(4), has the largest valence population, the smallest valence exponent, and the largest octupole term. Table 5 shows that the sharp octupole term on this atom is negative and oppositely-directed to those on N(5) and N(6), as was the case for the ring nitrogens.

### Conclusions

Because of the extensive and relatively accurate data set, the reasonably large unit cell, the hardness and thus low thermal motion of the crystal, and the existence of a non-crystallographic threefold rotor in the symmetry of the isolated molecule, the charge-density analysis of melamine has been particularly informative.

Larson & Cromer (1974) report on an analysis of the electron density of melamine with X-ray data alone. The valence-density-function model of Stewart (1973*a*) is used in the analysis, but the exponents are fixed at the standard molecular values. Multipoles are only included up to the quadrupole level, which means that the charge movement into the bonds of the heavy atoms is barely represented. To counteract this discrepancy they include 'bond-scattering' terms in some

analyses. Because of resolution problems and the absence of a core density, the hydrogen atom parameters are strongly correlated and could not be simultaneously refined. Larson & Cromer (1974) thus represent the hydrogen atom density by the monopole term only, and constrain the hydrogen atom thermal motion to be the anisotropic motion of the bonded nitrogen plus an isotropic term.

The only reflections considered observed were those for which  $I \geq 2\sigma(I)$ . It is to be expected that this practice, coupled with the capacity of the positional and thermal parameters to adjust for unaccounted charge density, should lead to rather low  $R$  factors. The  $R_w$  factor decreases from 0.043 at the 'standard least squares' level, to 0.037 at the 'scalars only' level, and to 0.033 with dipole and quadrupole terms included. The inclusion of nine bond-scattering terms results in a further decrease to 0.030. This model has 203 parameters, 96 more than in a standard least-squares refinement.

To compare their starting point with that of the present analysis, it would be necessary to know the  $R_w$  factor resulting from the zero-parameter model where the atomic scattering factors were used but the positions and thermal-motion parameters were held fixed at the neutron-determined values. Unfortunately this is not available but is expected to be somewhat greater than that of the standard molecular 'scalars

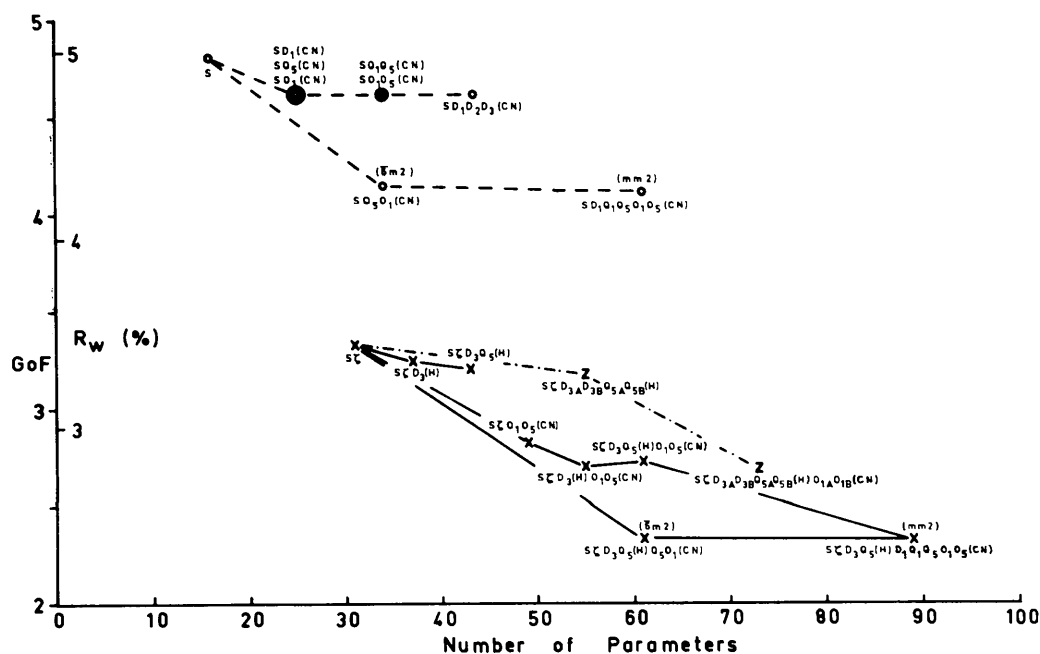


Fig. 4. The effect of exponent refinement and of inclusion of various multipoles in the model of fit to the data (GoF,  $R_w$ ). The model is characterized by which parameters are optimized. *S* refers to 'scalars' (a core and 15 valence populations),  $\zeta$  to the valence exponent, while the populations of the other multipoles are coded as in the text. The exponents for the *A* and *B* multipoles were defined in the text. The atoms on which the density functions were placed have their collective label [(H) or (CN)] following the multipole labels. Solid line (x): results with optimized exponents; dashed line (O): results with standard molecular exponents; chain-dotted line (Z): results with optimized scalar exponents and with the addition of the sharp multipoles.

only' analysis, which was 0.049. In the present analyses, then, the  $R_w$  factor decreases from around 0.06 at the isolated atom approximation, to 0.049 at the standard molecular 'scalars only' level, to 0.035 at the refined exponents 'scalars only' level, and finally to 0.024 at the  $\bar{6}m2$  level, and this with only 61 parameters. In addition to a lower  $R$  factor with fewer parameters, the present analysis reveals details of the charge density (such as that near the hydrogen atoms) not accessible to that of Larson & Cromer (1974). The deficiencies of this latter model show up most clearly in its estimates of the NH bond lengths, which vary from 0.73 to 0.83 Å. The neutron-determined values of Varghese, O'Connell & Maslen (1977) lie between 1.00 and 1.03 Å.

Most of the details of a later melamine analysis of Cromer, Larson & Stewart (1975*a,b*) are not known at the present time, but this refinement did include octupole terms and optimization of the exponents of the scalar terms (except on the hydrogens). The  $R_w$  factor was 0.0253 with 211 parameters. Once again the hydrogen charge density was poorly represented, resulting in underestimates of the NH bond lengths.

As in the diamond (Stewart, 1973*b*) and triazine analyses (Price, Maslen & Delaney, 1978), the exponent refinement is necessary for an adequate description of the valence density. In Fig. 4 the variation of the GoF and  $R_w$  parameters with the addition of various terms to the model is shown. The importance of exponent optimization and of the inclusion of the octupole term  $O_1$  on the heavy atoms is evident.

The projection coefficient, which is a measure of the space-filling properties of the density functions used, is expected to approach unity as the model approaches reality. In the analyses with standard molecular exponents, it has values of 1.08, 1.06 and 1.04 at the scalar-only,  $\bar{6}m2$  and  $mm2$  levels respectively. In the exponent-refinement analyses, these values are 1.06, 0.988 and 0.985 respectively.

The values determined for the exponents depend on the level of symmetry used. The mean carbon atom exponents, for example, are 1.680 (5), 1.610 (9) and 1.574 (4) bohr<sup>-1</sup> for the three levels of refinement. There is an inverse correlation between the valence populations and exponents, which suggests that a well-determined parameter is the height of the maximum of the density function. The values obtained for the exponents are in good agreement with those reported by Cromer, Larson & Stewart (1975*b*) at the same level of analysis. The carbon exponents were 1.63 (1) bohr<sup>-1</sup>. Those of the nitrogens, which were constrained to be equal, were 1.90 (1) bohr<sup>-1</sup>.

A comparison of Table 1 with Tables 3 and 4 shows that the agreement between the theoretical (Mulliken) populations and the experimental values is better for the 'scalars only' and ' $\bar{6}m2$ ' analyses than for the  $mm2$  analysis. Comparing these experimental numbers with those from the calculations, it is seen that the STO-3G

(SM) values for the carbon atoms agree better than those of the INDO treatment, but that the INDO values are better for the nitrogen atoms. The effect of hydrogen-bonding and intermolecular forces on the populations is much smaller in terms of the CNDO/2 (crystal) analysis of Santry (1974) than in the experimental analysis. These differences will be discussed in a later paper.

The charge-distortion terms represented by multipoles in the various refinements are in agreement with classical chemical concepts on bonding, and are well-defined and comparable within each group of like atoms. The analyses show that the ring nitrogens are more diffuse than the amine nitrogens. The bond-directed octupole term,  $O_1$ , has a larger population (at the  $\bar{6}m2$  level) for the nitrogen atoms than for the carbon atoms. There is a significant flattening of the charge cloud of the atoms of the ring, with electron density moving into the plane of the ring. There is no such effect on the amine nitrogen atoms. The effect is largest for the carbon atoms.

There are significant populations of dipole terms of high exponent (10 bohr<sup>-1</sup>) on the hydrogen atoms. These sharp dipoles are directed along the bond direction and are correlated with the bond-stretching vibration amplitude. Such terms may be an indication of the failure of the convolution (perfectly following atomic densities, or rigid pseudo-atom) approximation.

Only the carbon atom population parameters agree within the standard errors. The variation of parameters amongst the atoms within each of the other groups is strongly correlated with the hydrogen-bonding scheme. The information of Tables 6 and 8 shows that the effect of hydrogen bonding is to make the charge density near the hydrogen atom more diffuse, to lower the charge density in the vicinity of the nucleus, to decrease the polarity of the hydrogen charge cloud in the NH bond and to cause the charge cloud to spread out along the NH...N direction. The interatomic potential is flattened slightly in the NH...N direction, and steepened slightly (the hydrogen bond 'ties the H atom down' a little) in the perpendicular direction. This results in slightly longer NH bonds and larger bond-stretching thermal motion, but smaller vibrations in the perpendicular direction than is the case for the non-hydrogen-bonded H atoms. The increased vibration in the bond direction results in a larger apparent sharp dipole term in the density, caused by the inadequacy of the convolution approximation.

The final GoF of 2.33 (3) is still larger than unity. To some extent this discrepancy will be a consequence of the use of unrealistic (too small) errors on the observed structure factors. The errors used were from counting statistics alone. The use of the correct errors might result in a reduction of the GoF to about 1.5. The experience of a diamond-powder neutron data analysis (Price, Maslen & Moore, 1978) suggests that the use of the Becker & Coppens (1974) extinction

treatment may lower the GoF significantly. Corrections for thermal diffuse scattering (Helmholdt & Vos, 1975) may also be important. To what extent these changes in data reduction will affect the charge-density parameters is uncertain but it may well be that the resolution of the bonding-density features could be further improved.

This work has been supported financially by the Australian Research Grants Committee, by the Australian Institute of Nuclear Science and Engineering, and by the Research Committee of the University of Western Australia. Two of us (PFP and JNV) gratefully acknowledge receipt of Commonwealth Postgraduate Awards.

### References

- BACON, J. & SANTRY, D. P. (1971). *J. Chem. Phys.* **55**, 3743–3751.
- BECKER, P. J. (1975). *Acta Cryst.* **A31**, S227.
- BECKER, P. J. & COPPENS, P. (1974). *Acta Cryst.* **A30**, 129–149.
- CHANDLER, G. S. & SPACKMAN, M. A. (1975). Private communication.
- CLEMENTI, E. (1965). *IBM J. Res. Dev.* **9**, Suppl. *Tables of Atomic Functions*.
- COULSON, C. A. & THOMAS, M. W. (1971). *Acta Cryst.* **B27**, 1354–1359.
- CROMER, D. T., LARSON, A. C. & STEWART, R. F. (1975a). *Acta Cryst.* **A31**, S224.
- CROMER, D. T., LARSON, A. C. & STEWART, R. F. (1975b). *Application of Generalised Scattering Factors. How Atoms in Molecules Really Look*. Program Abstr., 33rd Pittsburgh Diffraction Conf.
- DELBAERE, L. T. J. & JAMES, M. N. G. (1973). *Acta Cryst.* **B29**, 2905–2912.
- EPSTEIN, J. & STEWART, R. F. (1975). *Electron Densities of Diatomic Hydrides from Generalised X-ray Scattering Factors*. Program Abstr. 33rd Pittsburgh Diffraction Conf.
- HEHRE, W. J., STEWART, R. F. & POPLE, J. A. (1969). *J. Chem. Phys.* **51**, 2657–2664.
- HELMHOLDT, R. B. & VOS, A. (1975). *Acta Cryst.* **A31**, S226.
- HUGHES, E. W. (1941). *J. Am. Chem. Soc.* **63**, 1731–1752.
- LARSON, A. C. & CROMER, D. T. (1974). *J. Chem. Phys.* **60**, 185–192.
- PRICE, P. F., MASLEN, E. N. & DELANEY, W. T. (1978). *Acta Cryst.* **A34**, 194–203.
- PRICE, P. F., MASLEN, E. N. & MOORE, F. H. (1978). *Acta Cryst.* **A34**, 173–183.
- SANTRY, D. P. (1974). Private communication.
- STEWART, R. F. (1972). *Electron Population Analysis with Generalised X-ray Scattering Factors*. Unpublished.
- STEWART, R. F. (1973a). *Acta Cryst.* **A29**, 602–605.
- STEWART, R. F. (1973b). *J. Chem. Phys.* **58**, 4430–4438.
- STEWART, R. F. (1974). *Charge Densities from X-ray Diffraction Data in Critical Evaluation of Chemical and Physical Structural Information*. pp. 540–555. New York: National Academy of Sciences.
- VARGHESE, J. N. (1974). Ph.D. Thesis, Univ. of Western Australia.
- VARGHESE, J. N., O'CONNELL, A. M. & MASLEN, E. N. (1977). *Acta Cryst.* **B33**, 2102–2108.
- ZACHARIASEN, W. (1967). *Acta Cryst.* **23**, 558–564.

*Acta Cryst.* (1978). **A34**, 216–223

## Pairs in $P2_1$ : Probability Distributions which Lead to Estimates of the Two-Phase Structure Seminvariants in the Vicinity of 0 or $\pi$

BY EDWARD A. GREEN AND HERBERT HAUPTMAN

*Medical Foundation of Buffalo, Inc., 73 High Street, Buffalo, New York 14203, USA*

(Received 16 May 1977; accepted 17 August 1977)

The first sequence of nested neighborhoods of the two-phase structure seminvariant  $\varphi_{12} = \varphi_{h_1 k_1} - \varphi_{h_2 k_2}$  in the space group  $P2_1$  is defined, and conditional probability distributions associated with the first four neighborhoods derived. In the favorable case that the variance of a distribution happens to be small, the distribution yields a particularly reliable value for  $\varphi_{12}$ . The most reliable estimates are obtained when  $\varphi_{12} \simeq 0$  or  $\pi$ .

### 1. Introduction

In the space group  $P2_1$ , the linear combination of two phases

$$\varphi_{12} = \varphi_{h_1 k_1} - \varphi_{h_2 k_2} \quad (1.1)$$

is a structure seminvariant if and only if

$$(h_1 - h_2, 0, l_1 - l_2) \equiv 0 \pmod{\omega_s} \quad (1.2)$$

where  $\omega_s$ , the seminvariant modulus in  $P2_1$ , is defined by

$$\omega_s = (2, 0, 2). \quad (1.3)$$

In short,  $\varphi_{12}$  is a structure seminvariant if and only if